American Mineralogist, Volume 72, pages 724–738, 1987

Modulated 2:1 layer silicates: Review, systematics, and predictions

STEPHEN GUGGENHEIM
Department of Geological Sciences, University of Illinois at Chicago, Chicago, Illinois 60680, U.S.A.
R. A. EGGLETON
Department of Geology, Australian National University, P.O. Box 4, Canberra, A.C.T. 2600, Australia

ABSTRACT

A continuous or nearly continuous octahedral sheet places important constraints on the geometry and topology of the attached tetrahedra in modulated 2:1 layer silicates. A plot of the average radius size of the tetrahedral cations vs. the average radius size of the octahedral cations shows the distribution of structures with respect to misfit of tetrahedral and octahedral (T-O) sheets, with modulated structures forming when misfit is large. It is tentatively concluded that such misfit is a requirement for modulated structures to form. It is evident that misfit of T-O sheets is a limiting factor for geometrical stability. On the basis of tetrahedral topology, modulated 2:1 layer silicates are divided into two major categories, islandlike (e.g., zussmanite, stilpnomelane) and striplike (e.g., minnesotaite, ganophyllite) structures. Bannisterite, which is more complex, most closely approximates islandlike structures. The plot involving cation radii is useful as a predictive tool to identify modulated structures, and parasettensite and gonyerite are identified as possible new members of the group. Diffraction data suggest that parsettensite has a variation of the stilpnomelane structure with smaller islandlike regions and gonyerite has a modulated chlorite structure.

Chemical mechanisms to eliminate misfit of T-O sheets usually involve Al substitutions. Because modulated 2:1 layer silicates commonly occur in Al-deficient environments, structural mechanisms are usually a requirement to eliminate misfit of component sheets. Besides a modulated tetrahedral sheet, structural mechanisms include (1) a limited corrugation of the interface between the T-O sheets that allows for a continuously varying structural adjustment, (2) distortions of the octahedral-anion arrangement located at strip or island edges, and, at least in one case, (3) cation ordering.

Near end-member compositions, modulated 2:1 layer silicates usually have Al in tetrahedral coordination, when Al is present, rather than in octahedral sites. It is concluded that a continuous edge-sharing octahedral sheet with large cations has a constraining influence on the size of possible substituting cations. This effect may explain the lack of octahedral ordering schemes in hydroxyl-rich micas where a small cation might occupy the M(1) site and a large cation might occupy the M(2) sites that surrounded M(1).

INTRODUCTION

Silicates in which SiO_4 tetrahedra are linked by sharing three corners to form infinite two-dimensional sheets constitute a major category of rock-forming minerals known as the layer silicates. Pauling (1930) outlined the general features of the micas and related layer-silicate minerals. These features usually include a layer comprised of two types of sheets; octahedrally coordinated cations form a sheet by sharing edges, and tetrahedrally coordinated cations form a sheet by sharing corners. If two tetrahedral sheets oppose each other with the octahedral sheet between, then a 2:1 layer is described, whereas if only one tetrahedral sheet is linked to the octahedra, the result is a 1:1 layer. The former layer type is common to the talc-pyrophyllite, mica, smectite, vermiculite, and chlorite groups, and the latter is found in the serpentine-kaolin group. Except in the talc-pyrophyllite and the serpentine-kaolin groups, adjacent layers may be separated by cations, hydrated cations, metal-hydroxyl octahedral sheets, organic compounds, or various other interlayer material.

The generalized model for 1:1 and 2:1 layer silicates as outlined by Pauling was firmly established by later workers. However, Zussman (1954) found that such a model does not hold in all cases. For example, the serpentine antigorite (Zussman, 1954; Kunze, 1956) shows an inversion and relinkage of tetrahedral apices across the ideally vacant regions between 1:1 layers. Since that time, the serpentine-like minerals caryopilite (Guggenheim et al., 1982), and greenalite (Guggenheim et al., 1982), the talc-like mineral minnesotaite (Guggenheim and Eggleton, 1986a), and the mica-like minerals zussmanite

0003–004X/87/0708–0724$02.00

(Lopes-Vieira and Zussman, 1969), stilpnomelane (Eggleton, 1972), ganophyllite (Eggleton and Guggenheim, 1986), and bannisterite (Threadgold, 1979) have been described as modulated structures based on the ideal structures of serpentine, talc, or mica. The recent structure refinement of pyrosmalite (Kato and Takéuchi, 1983) indicates that this structure may be classified as modulated, although its derivation directly from the traditional layer-silicate group is more complex.

We define a modulated layer silicate as one in which a periodic perturbation occurs in the structure. Often, this means that a superlattice forms. Although a prominent sublattice is present that approximates that of a normal type of layer silicate such as a serpentine, talc, mica, etc., the overall structure is more complicated and may involve tetrahedral connections across the interlayer region and/or discontinuities in the component sheets. For the purpose of this paper, we do not consider modulated layer-silicate structures to include those structures with discontinuities *and* out-of-plane displacements in the octahedral sheet because such displacements disrupt the two-dimensional layerlike aspects of the structure. Therefore, the minerals sepiolite and palygorskite are not discussed further because of their prominent octahedral discontinuities. The serpentine-like mineral chrysotile (Jagodzinski and Kunze, 1954; Whittaker, 1956a, 1956b) is not a modulated structure by the above definition, although its structure is based on principles similar to those outlined below.

A continuous or nearly continuous octahedral sheet places important constraints on the geometry and topology of an attached tetrahedral sheet. The purpose of this paper is to explore the relationship between the tetrahedral and octahedral sheets by reviewing previous concepts and by establishing a simple graphical approach to determine topological limits. Such limits are potentially useful as a predictive tool to determine not only which minerals require further study, but also to place constraints on the extent of structural adjustment.

The tetrahedral-octahedral relationship: Review of concepts

The tetrahedral sheet forms an ideally hexagonal network with tetrahedra containing primarily Si and possibly lesser amounts of Al^{3+} or Fe^{3+}. Each tetrahedron is linked to three other tetrahedral neighbors through shared corners, with these shared anions forming a *basal plane.* The fourth corner or *apical* oxygen is directed away from the basal plane and is involved also in the linkage to the octahedral sheet. The hexagonal model as described consists of sixfold tetrahedral rings forming a two-dimensional network. However, the *tetrahedral sheet* consists also of a hydroxyl (OH) group located at the same level as the apical oxygen and centered in the hexagonal ring. Therefore, the apical oxygens and OH groups form a complete plane of anions. Larger cations reside on another plane immediately adjacent to this anion plane and are coordinated to one OH group and two adjacent apical oxygens to form the lower portion of the *octahedral sheet.* To complete the octahedral sheet in 2:1 layer structures, a second tetrahedral sheet is inverted to oppose the first so that a similar configuration of apical oxygens and OH groups surround the octahedral cation. In 1:1 layer structures, the octahedral cations complete their sixfold coordination with OH groups only, which form an additional anion plane on one side of the octahedral cations and which are not shared with the tetrahedral sheet.

TABLE 1. Calculated and observed lateral dimensions of octahedral and tetrahedral sheets

Composition	Mineral	b_o (Å)	b_c (Å)
	Octahedral sheet		
$Al(OH)_3$	Gibbsite, bayerite	8.684, 8.672	8.125
$Mg(OH)_2$	Brucite	9.425–9.441	8.910
$Fe(OH)_2$	Synthetic	9.786	9.164
$Mn(OH)_2$	Synthetic	9.948	9.376
	Tetrahedral sheet		
Si_4O_{10}	None	—	9.15
$(Si_3Al)O_{10}$	None	—	9.335

Note: Observed *b*-axis dimensions, b_o, are from Saalfeld and Wedde (1974), Zigan et al. (1978), Zigan and Rothbauer (1967), and Oswald and Asper (1977). Calculated values, b_c, are from Eqs. 1 and 2 of text using ionic radii from Shannon (1976).

It is emphasized that the tetrahedral sheet is composed of three planes: the basal plane, the tetrahedral cation plane (usually Si) and the apical oxygen + OH plane. This latter plane forms a common junction between the two sheets and requires that the lateral dimensions of an octahedral sheet be equal to the lateral dimensions of the attached tetrahedral sheet. In addition to overall charge balance, this relationship represents the major constraint to variations in chemistry in both octahedral and tetrahedral sheets.

The degree of fit between the tetrahedral and octahedral sheets may be estimated (see, e.g., Radoslovich and Norrish, 1962) by comparing the lateral dimensions of the two component sheets in an unconstrained or free state. Lateral dimensions of the octahedral sheet may be estimated from the relation

$$b_{oct} = 3(\text{M–O})\sqrt{2}, \quad (1)$$

where M–O represents the mean octahedral cation to anion distance. Equation 1 assumes that the octahedra are regular. The octahedral lateral dimensions as calculated may be compared to naturally occurring octahedral sheets found as hydroxide minerals (Table 1). Calculated and observed values differ significantly and suggest the importance of octahedral distortions (e.g., Radoslovich, 1963) in determining the lateral dimension. For example, brucite has an observed *b*-cell length that is 6% larger then that calculated assuming no distortions.

Tetrahedral sheets do not occur in an unconstrained and free state, but it is possible to calculate an ideal lateral

extent based on (Si,Al) content from the equation

$$b(Si_{1-x}Al_x) \simeq 9.15 + 0.74x, \quad (2)$$

where x is the Al content. The assumptions are that the tetrahedral sheet is composed of hexagonal rings of tetrahedra, the tetrahedral angles are ideal, the Al–O distance is 1.748 Å, and the Si–O distance is 1.618 Å. The lateral dimensions of both component sheets will be identical in only certain special cases depending on the compositions of each sheet.

Common distortions affecting sheet sizes

Reducing relatively large tetrahedral sheets. The abundance of layer-silicate minerals with large variations in tetrahedral and octahedral composition suggests that there is a structural mechanism(s) that allows the tetrahedral and octahedral sheets to be congruent. The most important mechanism is distortion of the tetrahedral sheet by in-plane rotation of ajacent tetrahedra in opposite senses around the silicate ring (see, e.g., Guggenheim, 1984). This adjustment, known as "tetrahedral rotation," has been recognized in layer silicates since the 1950s (e.g., Newnham and Brindley, 1956). Tetrahedral rotation lowers the symmetry of the ring to ditrigonal and serves to reduce the lateral dimension of a larger tetrahedral sheet by as much as 10–12%.

Tetrahedral rotation (Radoslovich, 1961), as measured by the tetrahedral rotation angle α, is a common and effective means to reduce the lateral dimensions of a larger tetrahedral sheet to conform to the dimensions of an octahedral sheet. A less important distortion may involve the adjustment of the thickness of the sheet by compensating with a lateral dimensional change (Radoslovich and Norrish, 1962; Eggleton and Bailey, 1967). For example, the octahedral sheet may expand laterally by thinning or compressing individual octahedra. Such a distortion is measured by octahedral flattening (Donnay et al., 1964), which is described by the angle (ψ) between a line drawn perpendicular to the basal plane and a line joining opposite octahedral apices. By analogy, the tetrahedral sheet may deform in thickness to adjust its lateral dimension slightly. In this case, the measure of the tetrahedral deformation is τ, the mean of the O_{apical}–T–O_{basal} angles (Radoslovich and Norrish, 1962).

For many layer silicates with tetrahedral sheets larger than component octahedral sheets in the unconstrained state, ψ and τ parameters indicate octahedral-sheet thinning and tetrahedral-sheet thickening, respectively. Although these deformations are consistent with compensatory effects for sheet congruency (see Toraya, 1981), it is unlikely that such polyhedral distortions occur for this reason only. At least for cases of layer silicates with larger tetrahedral sheets, Lee and Guggenheim (1981) have shown that τ values are partly influenced by electrostatic repulsions of adjacent octahedral cations and the resulting shortening of shared edges with respect to unshared edges around the octahedron. It has been found that ψ values are influenced by similar repulsions (McCauley et al., 1973) and by field-strength effects (the ratio of valence to cation radius) of neighboring octahedra (Lin and Guggenheim, 1983). Additional contributing factors to ψ and τ values have been reported (cf., Hazen and Wones, 1972). *Clearly, the misfit between the two sheets is only one of several factors contributing to the magnitude of these parameters.*

Another notable distortion found in the octahedral sheet is the counterrotation of upper and lower oxygen triads (Newnham, 1961), designated as ω by Appelo (1978). Radoslovich (1963) suggested that shortened shared edges cause this effect, but regression analyses by Lin and Guggenheim (1983) indicate that the difference in size between the adjacent octahedral sites is the controlling factor. The results of the regression analyses imply that cation charge and shared-edge lengths are important insofar as they affect polyhedral sizes. For structures that have a uniform chemistry for all of the octahedral sites, variations in ω values between octahedra are negligible. However, octahedral-cation ordering will affect ω values, and the net effect of significant triad counterrotations reduces the lateral size of the octahedral sheet by up to a few percent.

Particularly in cases where there are two cation sites of unequal size, octahedral-cation ordering can affect the geometry of the tetrahedral sheet. For example, in micas that have a large or vacant M(1) site and two smaller M(2) sites, the tetrahedra tilt out of plane (Takéuchi, 1965) to accommodate the larger site. Such tilting forms a wave or corrugation of basal oxygens parallel to the direction of intralayer shift, e.g., the [110] direction in $2M_1$ polytypes and the [100] in 1M polytypes. The parameter Δz is often used in the literature to describe the z-coordinate deviation (in ångströms) between the oxygens located on the undulating basal-oxygen plane. It should be noted, however, that the effect of this distortion on the lateral dimensions of the tetrahedral sheet is negligible.

Enlarging relatively small tetrahedral sheets. For cases where the ideal tetrahedral sheet is smaller than the octahedral sheet, the variations in topology that allow congruency of the two sheet types are more severe. There is no single and simple mechanism, such as tetrahedral rotation, to minimize most of the misfit between the tetrahedral and the octahedral sheets. However, the origin of the misfit remains the same, and the tetrahedral and octahedral sheet sizes, therefore, should be correlated to the chemistry of both sheets.

Two previous attempts have been made to quantify the misfit between the tetrahedral and octahedral sheets. In examining 1:1 layer silicates, Bates (1959) defined a morphological index (M) on the basis of the average radius of cations occupying tetrahedral sites ($\bar{r}_t$) vs. the average octahedral-cation radius ($\bar{r}_o$). In a plot of $\bar{r}_t$ vs. $\bar{r}_o$, he defined an arbitrary line that represents a "best fit" of the component sheets and calculated the perpendicular distance away from this line as a measure of misfit. At the time, it was thought that misfit and morphology could be directly related in 1:1 structures, with platy serpentines

having the best fit and coiled, tubular, or cylinical serpentines having poor fit. However, Bates noted that misfit alone is not responsible for serpentine morhology, as the amount of H bonding between 1:1 layers plays an important, if not dominant, role. In addition, Guggenheim et al. (1982) have shown that there is no direct relationship between morphology and misfit, because Fe- and Mn-rich and Al-poor serpentines can be platy, although component-sheet misfit is large. Furthermore, Wicks and Whittaker (1975) have shown that there is compositional overlap between lizardite, chrysotile, and parachrysotile. Although a "morphological" index is perhaps an anachronism, the use of an average cation radius as a measure of misfit represents a valid and useful approach.

For Bates's (1959) analyses of morphology, assumptions as to the distribution of cations in the tetrahedral and octahedral sheets were not consequential. However, for an accurate measure of misfit, cation distribution between the component sheets is important. Also, as noted by Bates, interlayer bond strength, as determined by H bonding across the interlayer region, must be considered for 1:1 structures. In addition, Gillery (1959) and later workers (e.g., Steadman and Nuttall, 1963; Chernosky, 1975; Mellini, 1982) recognized that electrostatic interactions exist between 1:1 layers when, because of cation substitutions, the octahedral sheet acquires a positive charge and the tetrahedral sheet a negative charge, although the resultant 1:1 layer charge is neutral. Therefore, a misfit index based merely on $\bar{r}_o$ and $\bar{r}_t$ should not be used for the serpentines, which have an interlayer bond strength determined on the basis of the number and orientation of H bonds and on other electrostatic interactions.

Takéuchi (1965) suggested a direct measure (D) of misfit. This may be calculated from the formula: $D = (l_o - l_t)/l_o$ where l_t is the hexagon edge length formed by apical oxygens of a tetrahedral ring of *ideal hexagonal symmetry,* and l_o is the corresponding edge in the observed octahedral sheet. For a mica structure with both M(1) and M(2) sites equal in size and shape, l_o is equal to one side of the upper (or lower) oxygen triad of the octahedron. For trioctahedral micas, negative values of D indicate that the lateral dimensions of the tetrahedral sheet are greater than the lateral dimensions of the octahedral sheet. Presumably, tetrahedral in-plane rotation can readily compensate for this type of sheet misfit. Takéuchi (1965) discussed the parameter in dioctahedral micas, but of more interest for the discussion here is the case where D is positive and the octahedral sheet is larger than the tetrahedral sheet.

The concept of the direct measure of misfit, D, suffers from not being useful as a predictive tool. For an accurate analysis of l_t and l_o, it is first necessary to determine the structure. Alternatively, l_t and l_o may be calculated assuming ideal sheet geometries, but then the approach is only a gross approximation. For example, Takéuchi (1965) noted that talc has a D value of +2.0, suggesting that the tetrahedral and octahedral sheets do not match. Since then, the talc structure has been determined (Rayner and Brown, 1973) and refined precisely (Perdikatsis and Burzlaff, 1981). The misfit of the two sheets is eliminated by a tetrahedral sheet that is thinned considerably by distorting individual tetrahedra so that the lateral dimensions of the sheet increase. Clearly, the use of ideal sheet geometries may be misleading. Also, the effect of chemical substitutions, either tetrahedrally or octahedrally, cannot easily be calculated by this approach.

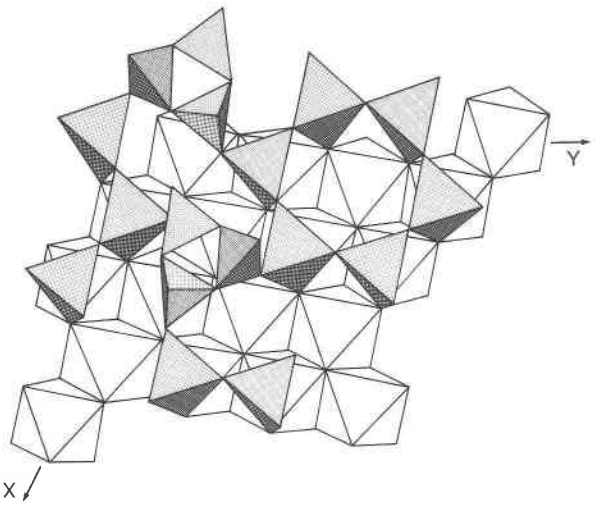

Fig. 1. A portion of the zussmanite structure viewed in perspective and with the K cations omitted. These cations occupy twelvefold sites between opposing sixfold rings, one of which is illustrated. (Modified from Lopes-Vieira and Zussman, 1969.)

Modulated 2:1 layer silicate structures

The modulated 2:1 layer silicate structures may be separated into two groups, (1) those having strips composed of tetrahedral rings on both sides of the continuous octahedral sheet and (2) those having regions of tetrahedral rings that are analogous to islands. Zussmanite and stilpnomelane belong to the latter whereas minnesotaite and ganophyllite comprise the former. Bannisterite does not clearly belong to either group but, for convenience, it has been included with zussmanite and stilpnomelane.

Island structures

Zussmanite. Zussmanite was described briefly by Agrell et al. (1965) who proposed a chemical formula of $(K_{0.92}Na_{0.07})(Fe^{2+}_{10.85}Mg_{1.53}Mn_{0.46}Al_{0.34}Fe^{3+}_{0.11}Ti_{0.01})_{\Sigma=13}(Si_{16.6}Al_{1.4})O_{42.2}(OH)_{13.8}$ (ideally, $KFe_{13}(Si_{17}Al)O_{42}(OH)_{14}$). Lopes-Vieira and Zussman (1969) determined and refined the structure of zussmanite in space group $R3$, but noted also that many reflections were streaked parallel to Z^*. Jefferson (1976) showed that these reflections were caused by two types of stacking disorder, one involving the rhombohedral structure and the other relating to a severely strained structure with triclinic symmetry. There is an apparent compositional variation between the two struc-

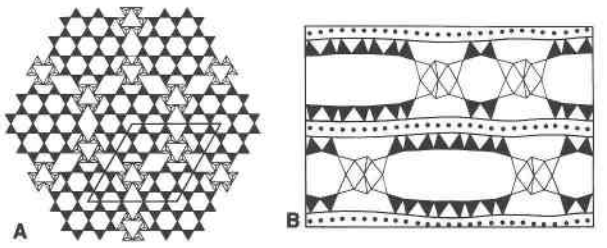

Fig. 2. An idealized stilpnomelane structure (A) projected onto the X-Y plane and (B) viewed along [110] (both modified from Eggleton, 1972).

tures with the triclinic form depleted in K and slightly enriched in Mn at the expense of Fe. Polytypes may form with both structures, and Jefferson (1976) has noted the occurrence of numerous one- and two-layer varieties. Muir Wood (1980), in a study on the same material, did not find the inverse K to Mn variation in all cases, as was reported by Jefferson (1976). In addition, he noted the occurrence of zussmanite-like (designated as "Zu2") material with cell parameters approximately 8% smaller and with a chemistry of approximately $KAlMn_{3-5}Fe^{2+}_{10-8}Si_{17}O_{42}(OH)_{14}$, by analogy to zussmanite.

The zussmanite structure (Lopes-Vieira and Zussman, 1969) contains T–O–T layers defined by sixfold rings of tetrahedra opposing a continuous octahedral sheet. Threefold tetrahedral rings laterally connect the six-fold rings and connect adjacent T–O–T layers through a tetrahedral edge across what is the interlayer region in a normal layer silicate (see Fig. 1). Alkali ions reside in the hole formed by two opposing sixfold rings in the interlayer region, but the number of such sites is restricted by the presence of the threefold rings; there are only one-fourth as many alkali positions in zussmanite as compared to a normal mica.

Stilpnomelane. Modern structural work on stilpnomelane was initiated by Eggleton and Bailey (1965) in which the subcell was defined and described. Eggleton (1972) described the full cell and later (Eggleton and Chappell, 1978) compared chemistry to physical properties and cell data. Crawford et al. (1977) found evidence for two two-layer and many long-range periodicities from an electron-microscope study.

Stilpnomelane is generally recognized as a group of minerals, with the bulk of component Fe ranging from primarily Fe^{2+} (*ferrostilpnomelane*) to primarily Fe^{3+} (*ferristilpnomelane*). Although Mg-dominant stilpnomelanes have been known for some time, Dunn et al. (1984) designated this species as *lennilenapeite*. A Mn-dominant species is known as *parsettensite*. (See Predicting Modulated Structures, p. 735.) The end-member Fe varieties have structural formulae dependent on the protonization of the hydroxyl groups: $K_5Fe^{2+}_{48}(Si_{63}Al_9)O_{168}(OH)_{48}\cdot 12H_2O$ for ferrostilpnomelane and $K_5Fe^{3+}_{48}(Si_{63}Al_9)O_{216}\cdot 36H_2O$ for ferristilpnomelane. Eggleton and Chappell (1978) have suggested a simplified formula based on one-eighth of the structural formula so that, for example, ferrostilpnomelane can be represented approximately by $K_{0.6}Fe_6(Si_8Al)(O,OH)_{27}\cdot 2H_2O$.

The structure of stilpnomelane (Eggleton, 1972) is composed of a continuous octahedral sheet and modulated tetrahedral sheets (see Fig. 2). The tetrahedral sheets articulate to the octahedral sheet, but form nearly trigonal islands of six-member hexagonal rings of SiO_4 tetrahedra. Each island consists of seven complete six-member silicate rings and has a diameter of seven tetrahedra. The islands are separated and linked laterally by an inverted single six-member silicate ring. In contrast to the hexagonal rings within the islands, these rings have a more trigonal configuration. In a normal layer silicate, the interlayer space is vacant or contains the alkali cation. In stilpnomelane, the interlayer region contains the alkali cation and the inverted six-member trigonal silicate rings, which link the islands and adjacent layers across the interlayer space. The interlayer has two trigonal rings joined along Z through the apical oxygens and a resultant d_{001} value of 12.2 Å.

Bannisterite. Smith (1948) and Smith and Frondel (1968) recognized that two different minerals had been confused for ganophyllite. Smith and Frondel (1968) presented X-ray, chemical, and additional optical data for bannisterite that established it as a species in its own right. Threadgold (1979) presented a structural formula based on electron-microprobe analysis and a refinement of the structure. However, full details have not yet been presented. Dunn et al. (1981) chemically analyzed material from Franklin, New Jersey, and Plimer (1977) reported on material from Broken Hill. Chemical formulae appear to range from $Ca_{0.45}(K_{0.32}Na_{0.19})(Fe_{5.1}Mn_{4.8}Mg_{0.1})_{\Sigma=10}(Si_{14.4}Al_{1.6})_{\Sigma=16}O_{38}(OH)_8\cdot 2(H_2O)$ for the Broken Hill material (Treadgold, pers. comm.) to $Ca_{0.43}(K_{0.41}Na_{0.055})(Fe_{1.46}Mn_{6.105}Mg_{1.425}Zn_{1.045}Fe^{3+}_{0.13})_{\Sigma=10.165}(Si_{14.27}Al_{1.53}Fe^{3+}_{0.20})_{\Sigma=16}O_{38}(OH)_8\cdot 6.1(H_2O)$ for the Franklin material (Dunn et al., 1981) with a structural formula of $K_{0.5}Ca_{0.5}M_{10}T_{16}O_{38}(OH)_8(H_2O)_{2-6}$ where M and T are the octahedral and tetrahedral cations, respectively.

Bannisterite (Threadgold, 1979) has a two-layer structure with one-quarter of the tetrahedra inverted toward the interlayer space. These tetrahedra share their apical oxygens with similarly inverted tetrahedra from adjacent layers. Sixfold rings are composed of tetrahedra that coordinate directly to the octahedral sheet. Fivefold rings, very distorted sixfold rings, and sevenfold rings are formed also, but each of these rings contains two inverted tetrahedra (Threadgold, pers. comm.). In this way, the close proximity of highly charged tetrahedral cations is eliminated in the fivefold and distorted sixfold rings. Similar fivefold and distorted sixfold rings are found in ganophyllite.

Strip structures

Minnesotaite. Gruner (1944) suggested that minnesotaite was the Fe^{2+} analogue of talc on the basis of X-ray powder photographs of impure material. However, although the d_{001} value of approximately 9.6 Å suggests a

talc structure, Guggenheim and Bailey (1982) concluded from single-crystal photographs of a twinned crystal that the structure is modulated. Further X-ray analysis and a chemical and transmission-electron microscopy (TEM) study by Guggenheim and Eggleton (1986a) supported this conclusion and outlined the details of the structure.

Guggenheim and Eggleton (1986a) showed that minnesotaite crystallizes in two structural forms, which may be designated *P* and *C* in accord with the Bravais lattice of the two respective unit cells. Crystallization of the structural forms appears to be related to chemistry, and the resulting misfit between the tetrahedral and octahedral sheets. A simplified structural formula for the *C*-centered cell using the chemical data of Blake (1965) and Guggenheim and Eggleton (1986a) on the basis of eleven oxygens is $(Fe_{2.50}Mn_{0.06}Mg_{0.39}Al_{0.05})(Si_{3.88}Al_{0.12})O_{10}(OH)_{2.60}$. Of the seven specimens studied, this sample was the only *C*-centered example, and, furthermore, it was the only sample that crystallized suffciently well to be studied by single-crystal X-ray methods. Although the *P*-cell structure varied somewhat in composition, a representative chemistry is given by $(Fe_{1.89}Mn_{0.03}Mg_{1.07})(Si_{3.99}Al_{0.01})O_{10}(OH)_3$.

Like talc, minnesotaite has a continuous octahedral sheet. There are adjacent Si tetrahedra on either side of this sheet to form an approximate 2:1 layer (see Fig. 3). However, in contrast to talc, strips of linked hexagonal rings of tetrahedra are formed only parallel to *Y*. A discontinuity of the normal configuration of the tetrahedral sheet results along *X* because some of the tetrahedra invert partially (note Figs. 3a, 3b). These tetrahedra form a chain extending parallel to *Y* in the interlayer region. The chain serves to link the adjacent strips within the basal plane and also links adjacent strips across the interlayer space. The latter linkage is achieved through a tetrahedral edge (approximately 2.7 Å), which is dimensionally equivalent to the interlayer separation in a normal talc structure. In this way, the d_{001} value of minnesotaite closely approximates the predicted value of an Fe-rich talc. However, the bonding of adjacent layers across the interlayer region is much stronger in minnesotaite than the weak van der Waal bonding in a talc structure.

The disposition of the tetrahedral strips is such that strips superpose directly across the interlayer space, but are displaced parallel to *X* by one-half of a strip width across the octahedral sheet. In a normal 2:1 layer silicate, the octahedral sheet is held in tension between the two opposing tetrahedral sheets and, thus, is planar. In minnesotaite, the strip displacement across the octahedral sheet relaxes such tension and allows limited curving of the tetrahedral-octahedral interface to produce a wavelike structure.

Tetrahedral strip widths in minnesotaite are dependent on the component sheet chemistry. Hence, there are variations in unit-cell size and symmetry. As the cations in the tetrahedra are essentially all Si, variations in octahedral-sheet chemistry are the most critical. When the octahedral sheet is relatively small, as in the Mg-enriched sheets, a modulation occurs every four tetrahedra along *X*, and ten tetrahedra (4 + 1 + 4 + 1) span nine octahedra; a *P* cell is produced. For the *C*-centered cell, strip widths alternate between three and four tetrahedra so that nine tetrahedra (4 + 1 + 3 + 1) span eight octahedra. The *C*-centered cell has been found only in the most Fe^{2+}-rich sample. A minnesotaite-like phase enriched in Mn was noted by Muir Wood (1980), but structural information is lacking.

Ganophyllite. The first careful optical study of ganophyllite was made by Smith (1948). He found evidence that the term "ganophyllite" was being applied to two separate layer silicates. Smith and Frondel (1968) differentiated these phases on the basis of X-ray data and designated them as ganophyllite and bannisterite (see above). The approximate chemical formula (Eggleton and Guggenheim, 1986) is $(K,Na,Ca)_6^{+7.56}(Mn,Fe,Mg)_{24}(Si_{32.5}Al_{7.5})O_{96}(OH)_{16}\cdot 21H_2O$ and Z = 8. Peacor et al. (1984) have given the name of *eggletonite* to samples with Na > K. Dunn et al. (1983) have found that for the limited number of samples they analyzed, there appears to be little variation in the octahedral occupancy.

Smith and Frondel (1968) showed that ganophyllite crystallizes in the monoclinic space group $A2/a$ with cell parameters $a = 16.60(5)$, $b = 27.04(8)$, $c = 50.34(15)$ Å, $\beta = 94.2(2)°$. There is a prominent monoclinic subcell with space group $I2/a$ and cell parameters $a_0 = 5.53 = a/3$, $b_0 = 13.52 = b/2$, $c_0 = 25.17$ Å $= c/2$, and $\beta = 94.2°$. Jefferson (1978) noted a triclinic polytype [$a = 16.54(5)$, $b = 54.30(9)$, $c = 28.52(8)$ Å, $\alpha = 127.5(3)°$, $\beta = 94.1(2)°$, $\gamma = 95.8(2)°$] in space group $|P\bar{1}$ or $P1|$ and interpreted variations in polytype as resulting from structural columns that can be stacked along {011} planes.

Kato (1980) determined the ganophyllite subcell structure by using single-crystal X-ray data. He described the subcell (note resemblances in Fig. 4) as having a continuous octahedral sheet with tetrahedral strips on both sides of the octahedra. The strips are three tetrahedral chains wide and are extended parallel to *X*. The strips are staggered across the octahedral sheet so that the rifts between strips are offset. The rift pattern allows a marked sinusoidal curvature of the octahedral sheet and of attached tetrahedra along *Y*. According to the Kato model, large alkali cations connect adjacent layers by occupying sites where rifts oppose each other across the interlayer.

Guggenheim and Eggleton (1986b) found that the large cations can be readily exchanged. These results are in contrast to the predicted behavior based on the Kato model. In that model, there is a high residual negative charge associated with the coordinating anions of the interlayer alkali site, thereby making cation exchange unlikely. Eggleton and Guggenheim (1986) re-examined the structure of ganophyllite using the Kato data set, several hundred additional weak reflections, and electron-diffraction data. They proposed a model (see Fig. 4) whose significant difference is based on the interlayer connectors. The triple-chain strips are connected by pairs of inverted tetrahedra that serve to connect both adjacent layers and neighboring strips. The alkali cations reside in the tunnels formed in

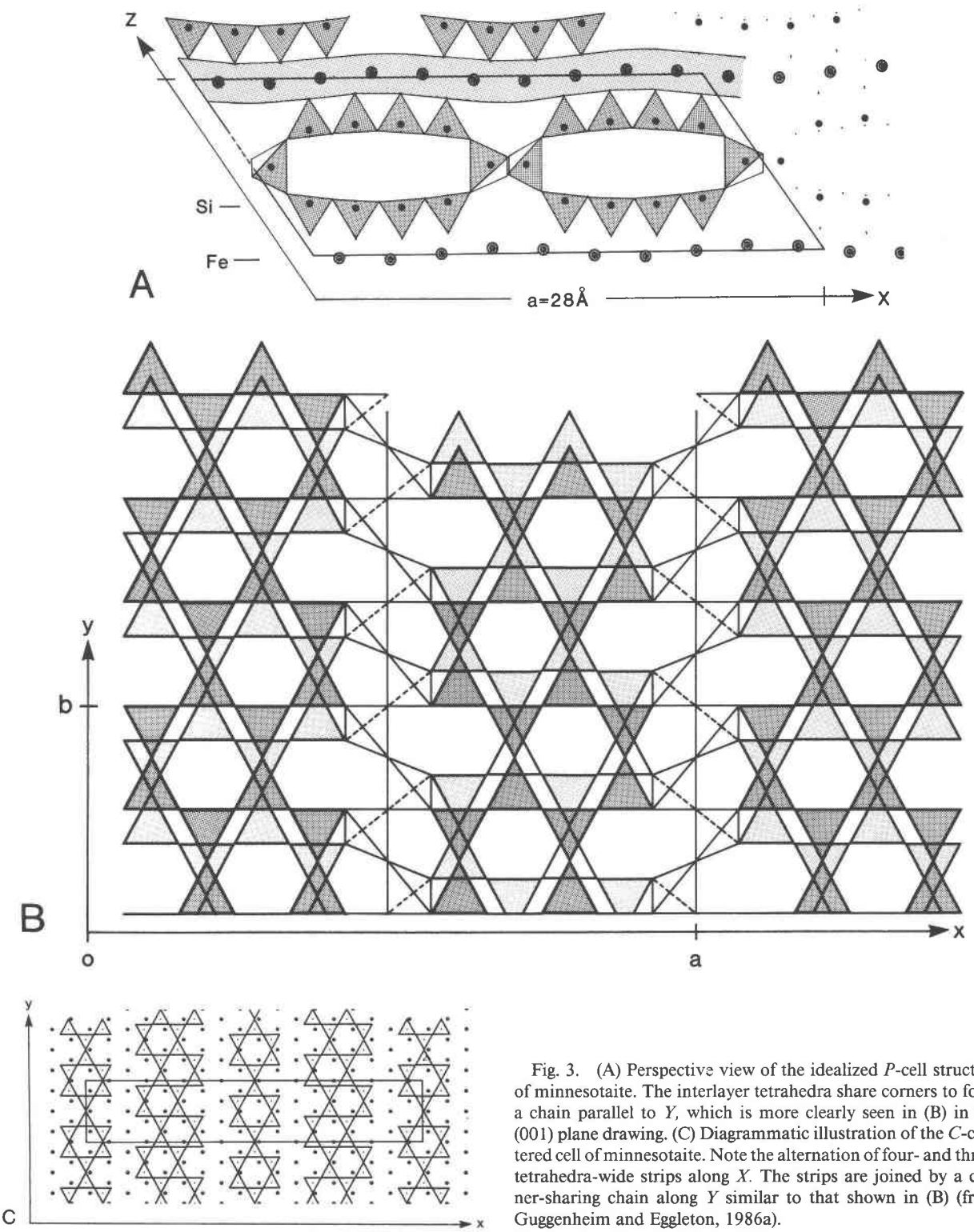

Fig. 3. (A) Perspective view of the idealized *P*-cell structure of minnesotaite. The interlayer tetrahedra share corners to form a chain parallel to *Y*, which is more clearly seen in (B) in the (001) plane drawing. (C) Diagrammatic illustration of the *C*-centered cell of minnesotaite. Note the alternation of four- and three-tetrahedra-wide strips along *X*. The strips are joined by a corner-sharing chain along *Y* similar to that shown in (B) (from Guggenheim and Eggleton, 1986a).

the "interlayer" region between the inverted tetrahedra. These sites are numerous and poorly defined and may be compared to the exchange-cation sites in zeolites. Overall, the structure may be classified as a modulated mica structure.

Discussion

Excessive out-of-plane tilting of tetrahedra as observed in the 1:1 layer silicate chrysotile (e.g., Whittaker, 1956b) cannot occur in normal 2:1 layer silicates; opposing tet-

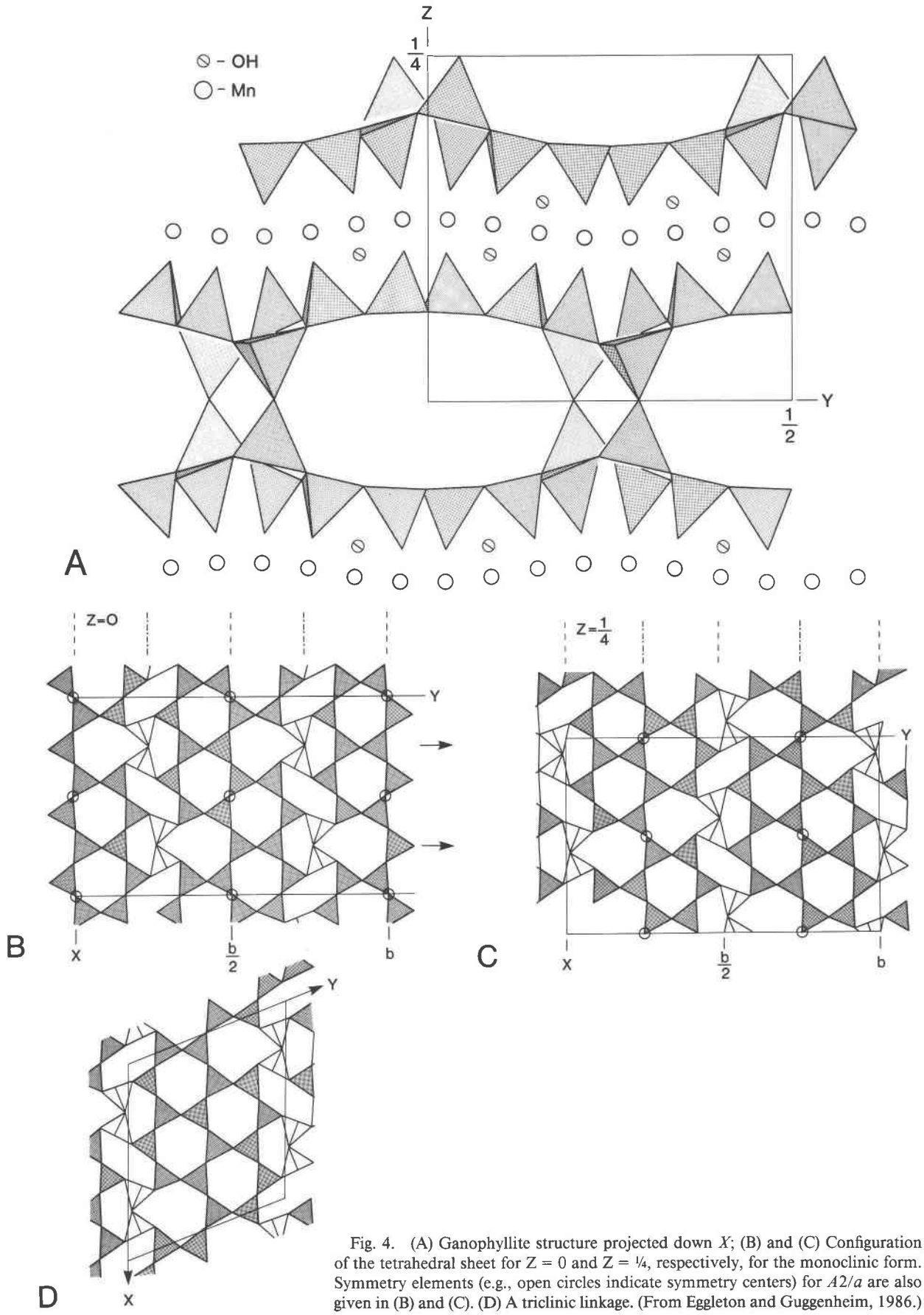

Fig. 4. (A) Ganophyllite structure projected down X; (B) and (C) Configuration of the tetrahedral sheet for Z = 0 and Z = ¼, respectively, for the monoclinic form. Symmetry elements (e.g., open circles indicate symmetry centers) for $A2/a$ are also given in (B) and (C). (D) A triclinic linkage. (From Eggleton and Guggenheim, 1986.)

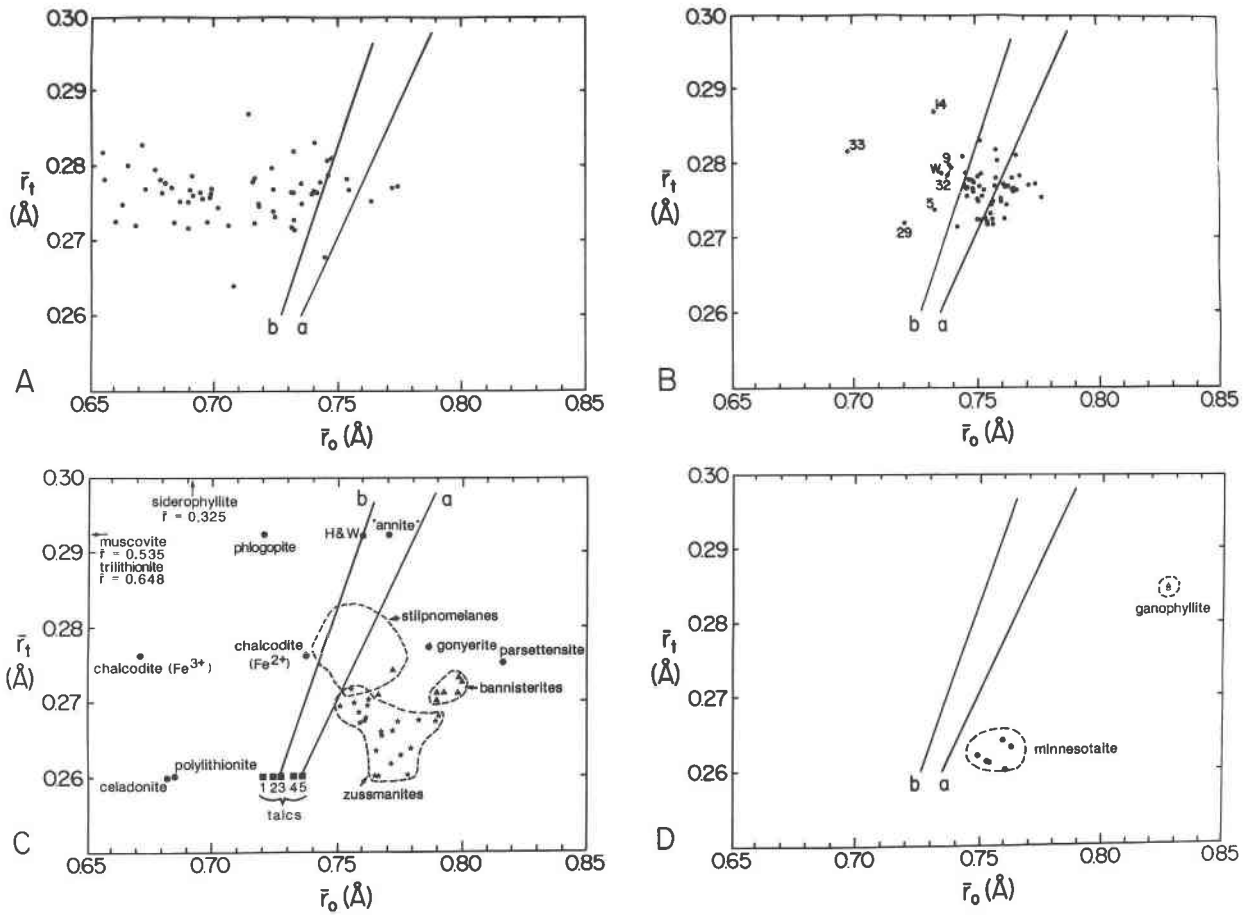

Fig. 5. A series of plots of the average radius of cations occupying the tetrahedral sites ($\bar{r}_t$) vs. the average radius of cations occupying the octahedral sites ($\bar{r}_o$) based on ionic radii from Shannon (1976) and observed compositions. Lines *a* and *b* are explained in the text, and octahedral vacancies are ignored in the calculations (see text, also). (A) and (B) Compositions of stilpnomelane with calculations based on reported Fe^{3+} values (A) or recalculated assuming that all Fe is Fe^{2+} (B). Chemical analyses are taken from Eggleton and Chappell (1978, Table 1), Eggleton (1972, Table IVa), and Dunn et al. (1984) and show a wide range of chemical variations. Labeled points refer to analyses in the original sources. (C) Confining compositional regions for islandlike structures for stilpnomelane (from Fig. 6B), zussmanite, and bannisterite and individual points for chalcodite, gonyerite, and parsettensite. These regions do not necessarily show maximum limits of geometrical stability. Boxes (labeled 1–5) are talc compositions for ideal (1) and Fe-rich talcs (2, Robinson and Chamberlain, 1984; 3, Forbes, 1969; 4, Lonsdale et al., 1980; 5, as no. 2 with all Fe as Fe^{2+}). Analyses: zussmanite, Muir Wood (1980, p. 614); bannisterite, Dunn et al. (1981), Threadgold (unpub.); and gonyerite, Frondel (1955). (D) Shows a plot analogous to (C), but for striplike structures. Analyses: minnesotaite, Guggenheim and Eggleton (1986a); ganophyllite, Eggleton and Guggenheim (1986).

rahedral sheets across a common octahedral sheet hold the octahedral sheet flat under tension. However, a limited corrugation in modulated 2:1 structures is possible because tension is relieved at the point of modulation where the tetrahedral inversions occur. It is noteworthy that the structure simulates a 1:1 layer silicate at these inversion points. Therefore, modulated 2:1 layer silicates involve a continuously varying structural adjustment that compensates for differences in component-sheet lateral dimensions. It is emphasized, however, that the corrugation is limited in range and that a configurational change involving tetrahedral inversions is a requirement.

Tetrahedral inversions usually involve "extra" tetrahedra that serve to span ever-increasing octahedral-sheet lateral dimensions. For example, the ratio of tetrahedral to octahedral cations increases from 1.33:1 in talc to 1.40:1 in zussmanite, 1.50:1 in stilpnomelane, 1.60:1 in bannisterite, and 1.67:1 in ganophyllite. These variations are a direct result of the tetrahedral configurational change and correspond to the large lateral size of the octahedral sheet.

The $\bar{r}_t$ vs. $\bar{r}_o$ plot

The use of $\bar{r}_t$ vs. $\bar{r}_o$ plots to delineate geometrical "stability" fields may be justified for the modulated 2:1 layer silicates. Obviously, the variations in the ratios of tetrahedral to octahedral cations and the structural compensation for differences in the lateral dimensions of the component sheets suggest the utility of such plots. Unlike the

1:1 layer silicates, the 2:1 layer silicates lack strong layer-to-layer interactions either through H bonding or by electrostatic interactions caused by cation substitutions. In contrast to the serpentines, tetrahedral sheets in the modulated 2:1 layer silicates face tetrahedral sheets across the interlayer. Also, in some cases, the layer-to-layer distances are quite large because of one or more tetrahedra involved in linkages across the interlayer region. Figure 5 shows a series of such plots, where $\bar{r}_t$ is the weighted-average tetrahedral-cation radius and $\bar{r}_o$ is the analogous parameter for the octahedral cations. Representative layer-silicate minerals have been plotted in Figure 5c using ionic radii data from Shannon (1976). In order to make the plot useful as a predictive tool (see below), octahedral vacancies are not included in the calculations, as the number of such vacancies would be unknown in an unknown structure.

A single line separating the region of geometrical stability of normal layer silicates from that of the modulated 2:1 layer silicates cannot be defined. Approximations can be made from theoretical considerations (line *a*) as calculated from Equations 1 and 2 and from experimental studies (line *b*) such as Hazen and Wones (1972) and Forbes (1969). Line *a* is based on the assumption that neither the octahedra nor the tetrahedra are distorted. Line *b* does not have this restriction but does suffer from the fact that experiments may not reflect conditions that maximize misfit. It is noteworthy that Fe-rich talcs (Robinson and Chamberlain, 1984; Lonsdale et al., 1980) plot generally between the extremes set by lines *a* and *b*. Guggenheim (unpub. data) has shown by TEM that these Fe-rich phases are true talcs and not minnesotaite structures. It is noteworthy also that the oxidation state for the Fe has not been characterized adquately in all cases. Furthermore, it is emphasized that these lines are approximations and that no sharp boundary delineating fields of geometrical stability has been determined. In part, these lines are approximations because the plot represents compositional effects only and does not consider the ionic radii of the cations at temperatures and pressures of formation. In addition, errors associated with composition and especially the oxidation state of Fe may be large. These and other considerations are discussed in more detail below.

The compositions of the modulated structures cluster to the right of line *a* and *b* with the notable exception of the stilpnomelanes (Fig. 5a). The large range of compositions for the stilpnomelanes may be a result of postcrystallization oxidation (see Hutton, 1938; Zen, 1960). Figures 5a and 5b show the effect of calculating $\bar{r}_o$ and $\bar{r}_t$ values based on both Fe^{3+} (0.65 Å) and Fe^{2+} (0.72 Å) values. With the exception of one analysis (no. 33), which is very Al-rich, all points falling to the left of line *b* have significant octahedral vacancies. If such vacancies (at a "radius" of 0.82 Å) are included in the $\bar{r}_o$ term, all these points would shift significantly to the right near line *b*. Ignoring octahedral vacancies in the $\bar{r}_o$ term produces a greater spread in points for the other plots in Figure 5 also. The conclusion that misfit between the tetrahedral and octahedral sheets is necessary to produce a modulated structure should be considered tentative until additional data are obtained for analysis no. 33. Clearly, however, misfit of tetrahedral and octahedral sheets is a geometrically *limiting* factor. Whereas (Fe^{2+},Fe^{3+}) stilpnomelanes may have a large compositional range, there is a geometrical limit in which the misfit between the two kinds of sheets prevents the formation of the structure (at higher average octahedral-cation sizes). It is noteworthy that all modulated structures have compositional regions that fall to the right of lines *a* or *b*, the two approximations for the limitation of the congruency of normal tetrahedral and octahedral sheets. Therefore, when compositions fall to the left of these lines, the modulated structure(s) requires readjustments that involve lateral reductions in the dimensions of the tetrahedral sheet, such as tetrahedral rotation or possibly sheet thinning or thickening, etc.

The use of the $\bar{r}_t$ vs. $\bar{r}_o$ plot requires that the chemistry, including the oxidation state of the constituent cations, has been determined and that the structural formula is known or known approximately. It is assumed that alkali cations have no or little effect on the linkage between the tetrahedral and the octahedral sheets. Of particular importance is the allocation of Al, which may commonly occur both tetrahedrally or octahedrally in layer silicates. However, examination of the *ideal* formulae of all modulated structures (see above) indicates that Al is tetrahedral. Examination of the chemical composition of natural phases suggests that Al occurs only in the tetrahedral site at end-member compositions, i.e., when the average octahedral-cation size is large relative to Al. This relationship suggests that there are geometric constraints involved.

Cation partitioning

In a continuous trioctahedral sheet, the octahedra share edges and thus have a constraining effect on the size of neighboring octahedra. In an octahedral sheet composed primarily of large cations, an isolated octahedron containing a much smaller cation will be unstable. This instability results from the larger shared edges between the octahedron containing a small cation and its six large octahedral neighbors; small cations do not usually reside in cavities that are too large. Therefore, for modulated layer silicates with primarily Fe^{2+} or Mn in the octahedral sheet, Al should prefer the tetrahedral sites. The differences in radii between neighboring Al^{3+} and Fe^{2+} (~30%) or Al^{3+} and Mn^{2+} (~35%) would effectively enlarge an Al octahedral site to an unacceptable degree. However, when sufficient Al^{3+} is present so that there is a coalescence of smaller-size octahedra, this effect is minimal and site assignment is more uncertain. It is also unclear whether the effect would be important for synthetic phases where equilibrium has not been acheived or for structures where the octahedral sheet is discontinuous, as cations could preferentially enter sites at sheet edges.

For an octahedral sheet composed of large cations, it is argued that an isolated octahedron containing a relatively

small cation will be avoided. Such an argument applies to all trioctahedral 2:1 layer silicates, including the hydroxyl-rich micas. For these micas, the general cation-ordering pattern (Guggenheim, 1984, p. 71) shows a trend of a larger M(1) site relative to M(2). In a typical mica, site M(1) is surrounded by six M(2) sites, whereas each M(2) site shares edges with three other M(2) sites and three M(1) sites. Thus, the M(1) may be considered "isolated" in the sense that it is sharing edges with only one type of octahedral site, M(2). Hence, the constraining effect of M(2) dictates that a smaller cation avoids entering M(1), as is generally observed.

There are several notable exceptions to the general ordering pattern, namely (1) clintonite (Takéuchi and Sadanaga, 1966), which has been described with a small M(1) site containing Al and relatively large M(2) sites containing Mg, and (2) some Li-rich micas (e.g., Guggenheim and Bailey, 1977; Guggenheim, 1981) with one small Al^{3+} octahedral site and two large sites. Recent neutron diffraction (Joswig et al., 1986) and X-ray diffraction studies (MacKinney and Bailey, in prep.) of clintonite suggest that the earlier work is in error and that clintonite does conform to the normal ordering pattern of a relatively large M(1) site. In the Li-rich micas, sufficient F, univalent cations, and vacancies exist to prevent a uniform geometry from developing in the octahedral sheet. For example, octahedral sites containing vacancies and univalent cations readily distort to accommodate their trivalent Al neighbor. Thus, they cannot act to constrain sizes of neighboring octahedral sites. Furthermore, F substitution for (OH) favors being associated with a smaller site (Guggenheim and Bailey, 1977).

More direct evidence that octahedra may effectively constrain the size of neighbors with shared edges has been given by computer modeling simulations by Baur et al. (1982) in the rutile-type structure. For this case it was found that a larger VF_6 octahedron would be reduced in size by about 0.25% if surrounded by smaller MgF_6 octahedra. Although rutile is composed of edge-sharing octahedra forming chains rather than sheets, it is clear that the argument is similar, and it would be expected that the effect is greater for a sheetlike arrangement.

Effect of temperature and pressure

The $\bar{r}_t$ vs. $\bar{r}_o$ plot requires precise values for ionic radii at the temperature and pressure of mineral formation, if the plot is to represent the true upper limits of misfit between the tetrahedral and octahedral sheets. However, not only are these values difficult to obtain, it is often difficult to ascertain the environmental conditions of mineral formation. Therefore, the regions of delineating geometric stability are only approximations, as the ionic radii used for these plots are based on ambient conditions.

High-temperature studies of fluorophlogopite (Takeda and Morosin, 1975) and high-pressure studies of phlogopite and chlorite (Hazen and Finger, 1978) have demonstrated strong anisotroic temperature and pressure responses that relate to differences in bonding within and between 2:1 layers. For example, interlayer distances are characterized by weaker bonds in these layer silicates. Therefore, interlayer-volume reduction is high when compressive forces are applied along Z^*. These results imply that hydrostatically applied stress to the system is not necessarily transmitted through the structure isotropically, but is generally controlled by and transmitted along bonds. In contrast, the inverse relationship generally holds for increasing temperature, with interlayer volume increasing greatly.

Unlike normal layer silicates, modulated 2:1 layer silicates have tetrahedral connectors across interlayer space and, therefore, should be significantly stiffer along Z^*. Thus, the interlayer region cannot act as an efficient pressure "buffer." Instead, the tetrahedral connectors would be expected to transmit pressure more efficiently along Z^*. Because the tetrahedra are very rigid, an octahedral site in a modulated structure would be expected to have a different compressibility than the analogous site in a normal layer silicate. Assuming that compressive forces are transmitted to the octahedral sites efficiently and are not greatly attenuated by T–O–T bending (see the suggestion by Vaughan in Hazen and Finger, 1982, p. 155–156), a high-pressure, low-temperature environment should effectively promote a reduced misfit of tetrahedral and octahedral sheets. These conditions apparently prevailed during the formation of zussmanite (Agrell et al., 1965), which is found in the Franciscan Formation of California and is believed to be of blueschist-facies origins. Of course, although misfit of tetrahedral and octahedral sheets may be a geometrically limiting feature of these structures, thermal stability is not based necessarily on this feature alone.

Modulations along preferred directions

Variations in the topological arrangement of the tetrahedra must have important consequences in how the misfit between the two sheets is relieved. Strip structures with tetrahedral strips offset on alternate sides of an octahedral sheet (e.g., see Fig. 3a or 4a) allow the octahedral sheet to be wavelike and, hence, allow the distance from apical oxygen to apical oxygen to increase. This increase results in tetrahedra tilting out of the (001) plane and effectively increases the lateral dimensions of the tetrahedral sheet. Furthermore, the change in the configuration of the sixfold ring relieves the strain along one axis. Whereas these mechanisms are suitable for relieving misfit in one direction, they do not explain why there is no modulation of the strip structure parallel to either Y as in minnesotaite or X as in ganophyllite, i.e., why is the hexagonal ring strip continuous? Eggleton and Guggenheim (1986) suggested that Al preferentially occupies the central continuous tetrahedral chain of the triple chain in ganophyllite. This substitution sufficiently increases the chain dimension so that it may span the octahedra along X. Evidence that this substitution occurs comes from (1) tetrahedral-site size considerations and (2) the position of the interlayer cation, which is located predominantly near the tet-

rahedral rings at the center of the strip. These tetrahedra would have undersaturated basal oxygens. Tetrahedral chains lateral to the central Al-bearing tetrahedral chain are lengthened by the addition of the inverted tetrahedra (see Fig. 4). Ganophyllite represents the first modulated layer silicate refined sufficiently to reveal that cation-ordering effects may play an important role in establishing the stability of a modulated 2:1 structure.

In minnesotaite, misfit of tetrahedral and octahedral sheets is relieved along the strip direction by distortions within the octahedral sheet (Guggenheim and Eggleton, 1986a). Apparently, the structure can accommodate greater misfit when strip edges are numerous because of narrow strip widths (three and four tetrahedra wide). The octahedra would have a greater ability to distort if the oxygen normally shared between both the tetrahedral and octahedral sheets is not constrained in its position. Tetrahedral inversions require that those oxygens are replaced by OH groups to complete the octahedral coordination about the Fe ions. Thus, the OH groups have greater positional freedom. However, it should be noted that there is no direct experimental evidence indicating such distortions, as the data were insufficient to accurately refine either the subcell or the supercell.

Island structures have a greater capacity for variations in chemistry than the strip structures. For example, in stilpnomelane, it would be expected that tetrahedral rotation would be the primary mechanism allowing such a diversity of compositions (see Fig. 5). Tetrahedral rotation requires a lateral shortening of the tetrahedral sheet with components along both X and Y. These directions are consistent for an island structure, but oppose the development of strip structures that require an extended chain in one direction. Limited tetrahedral rotation, however, is still possible in strip structures. For example, in ganophyllite, sufficient tetrahedral Al is present to overcompensate for the misfit in the strip direction.

In summary, it has been proposed that the concept of misfit of tetrahedral and octahedral sheets may be useful to delineate the upper limits of geometrically constrained structural stability for the modulated 2:1 layer silicates. However, it is necessary to know the mineral chemistry, including the oxidation states of the elements, in order to represent such limits effectively. Unless structural information is available or may be inferred correctly, it is suggested that Al be assigned to the tetrahedral sites, especially when the octahedral sheets are nearly end-member Fe^{2+}, Mn, or Fe^{2+} + Mn. Apparently, octahedral distortions, if they occur frequently, and cation ordering may act to relieve the misfit of tetrahedral and octahedral sheets. These structural variations may act together with the more obvious mechanisms (reversal of tetrahedral apices, the thinning or vertical expansion of the component sheets, or the limited curving of the tetrahedral-octahedral interface, etc.) to make the two sheets congruent. The effects of environmental conditions of formation are important also, as temperature and pressure are known to affect coordination polyhedra differently. With all of these known variables, it becomes of interest to determine if it is still possible to identify modulated structures from chemical considerations alone. Furthermore, it is useful to determine if it is possible to predict or construct reasonable models based on chemical or limited other data.

Predicting modulated structures

Eggleton has listed (Table IVb of Eggleton, 1972) analyses that do not seem to conform to the stilpnomelane structural model. Some of these analyses are old and possibly erroneous, whereas other have been clearly linked to structures that have been shown to be unrelated to stilpnomelane. Two analyses (no. 46–chalcodite and no. 39–parsettensite) deserve further comment. Chalcodite plots in Figure 5 within the stilpnomelane region if it is assumed to have a structural formula with 72 tetrahedral sites similar to stilpnomelane. It seems likely from the chemistry that chalcodite is a variety of stilpnomelane. Transmission-electron diffraction patterns of chalcodite from the Sterling mine, Antwerp, New York, show characteristic stilpnomelane patterns.

In contrast to chalcodite, parsettensite plots well away from the regions on the $\bar{r}_i$ vs. $\bar{r}_o$ plot (Fig. 5) for either island or strip structures. It should be noted that all Si, Al, and Fe were considered in fourfold coordination and that there is still a 0.8 cation deficiency if compared to a tetrahedral total of 72 cations per formula unit as in stilpnomelane. Likewise, there is a 0.8 octahedral-cation excess out of 48. Although the analysis is old (Jakob, 1923) and possibly suspect, the Mn-rich octahedral sheet suggests considerable misfit.

Figure 6 shows a transmission-electron diffraction pattern of the basal plane (electron beam parallel to Z^*) of parsettensite. The two-dimensional hexagonal or pseudohexagonal pattern is indicative of a layer structure with the more intense nodes derived from the strong scattering material of a continuous or nearly continuous octahedral sheet. Like most layer silicates, parsettensite shows perfect cleavage on the (001) plane. Weaker nodes, also in a hexagonal or pseudohexagonal arrangement, are caused by a modulated tetrahedral sheet. The hexagonallike nature of the basal plane suggests that the structure is islandlike, as a strip structure would show a superlattice along one direction only. X-ray powder-pattern photographs (not shown) suggest a possible analogy to the structure of stilpnomelane. However, it should be noted that different tetrahedral configurations solve similar magnitudes of misfit of the tetrahedral and octahedral sheets; for example, note the overlapping regions of stilpnomelane and zussmanite in Figure 5. At the same meeting in which portions of this paper were presented in oral form (Guggenheim, 1986), Ozawa et al. (1986) presented data on the unit cell of parsettensite, thereby independently confirming the modulated nature of parsettensite. They have defined a cell of a = 39.1 Å, b = 22.6 Å, and d_{001} = 12.6 Å.

It appears unusual that there have been no reports of a modulated chlorite structure, as all other layer-silicate groups are represented. Frondel (1955) reported an Al-

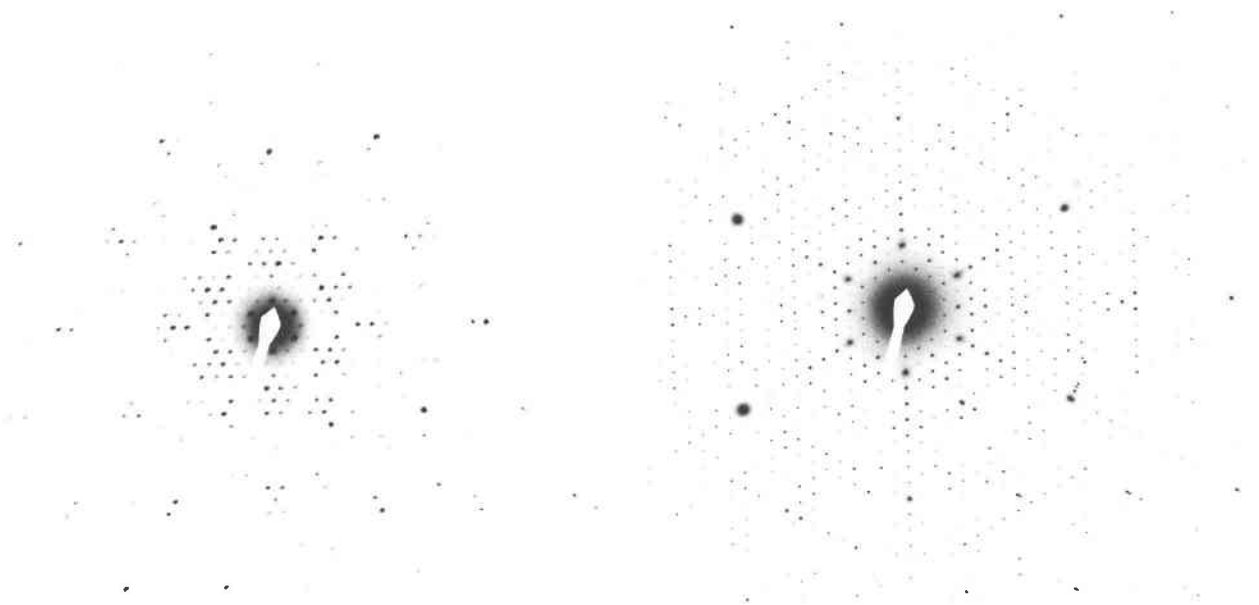

Fig. 6. Electron-diffraction pattern of the basal plane (beam parallel to Z^*) of parsettensite (left) compared to stilpnomelane (right).

poor, Fe- and Mn-rich chlorite known as gonyerite. If Si, Al, and Fe^{3+} are tetrahedrally located to conform to a chlorite structural formula (total tetrahedral occupancy of 4.0 cations per formula unit), the chemistry may be plotted on a $\bar{r}_t$ vs. $\bar{r}_o$ plot (Fig. 5). We emphasize, however, that the normal chlorite structure consists of two octahedral sheets, and it is likely that elemental partitioning can affect misfit in a chlorite. In addition, it is unclear how H bonding in the interlayer region may affect comparisons to other modulated structures. However, with these constraints and even if all small octahedral cations and all large tetrahedral cations are partitioned within the 2:1 layer, there is still considerable misfit.

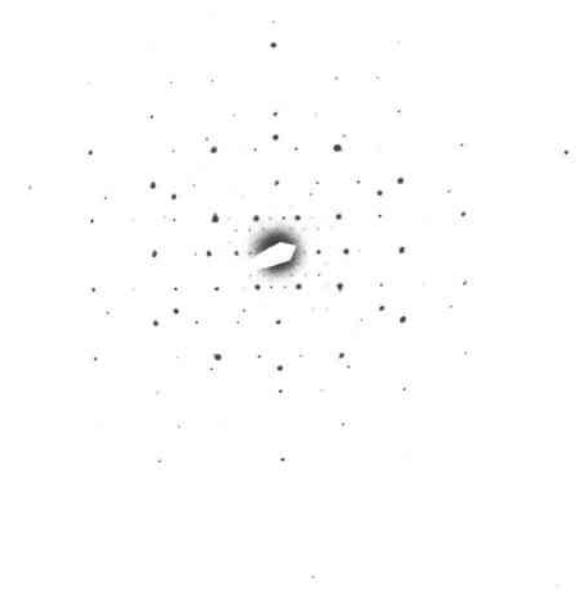

Fig. 7. Electron-diffraction pattern of the basal plane of gonyerite.

Examination of transmission-electron diffraction patterns of the gonyerite basal plane shows, in addition to reflections attributed to the heavy octahedral cations, weaker reflections indicating a superlattice presumably related to tetrahedral modulations (see Fig. 7). The lattice is based on a hexagonal cell indicating an islandlike structure. Diffraction data involving $00l$ reflections are consistent with a 28-Å c cell parameter. It is notable that patterns show strong l = odd reflections, and these reflections probably indicate that the (two-layer) unit cell is not composed of similar 2:1 layers. High-resolution transmission-electron microscopy (HRTEM) has confirmed this interpretation. Gonyerite is considerably more complex than a normal two-layer chlorite in which a two-layer sequence is a result of stacking variations. Because of the complexity of a chlorite structure, we would be premature to suggest a modulation description. Both the parsettensite and the gonyerite structures are to be described in more detail at a later time.

The possibility of using the plotted position (Fig. 5) of a modulated structure relative to lines a or b to predict the island size or strip width is limited. The nature of the tetrahedral perturbation at either the island or strip boundary, the extent of out-of-plane tetrahedral tilting, the possibility of cation ordering, etc., all serve to make such predictions on an a priori basis difficult. However, if additional information such as cell parameters or sys-

tematic variations in overall diffraction intensity is known, it is possible to construct possible models for the structure.

Acknowledgments

We thank S. W. Bailey, F. Wicks, and R. M. Hazen for reviewing the manuscript and M. Vaughan, University of Illinois at Chicago, for helpful discussions. We gratefully acknowledge the Research Resources Center of the University of Illinois at Chicago and B. Hyde, Australian National University, Canberra, Australia, for the use of the transmission-electron microscopes.

References

Agrell, S.O., Bown, M.G., and McKie, D. (1965) Deerite, howieite and zussmanite, three new minerals from the Franciscan of the Laytonville district, Mendocino Co., California (abs.). American Mineralogist, 50, 278.

Appelo, C.A. (1978) Layer deformation and crystal energy of micas and related minerals. I. Structural models for 1M and $2M_1$ polytypes. American Mineralogist, 63, 782–792.

Bates, T.F. (1959) Morphology and crystal chemistry of 1:1 layer lattice silicates. American Mineralogist, 44, 78–114.

Baur, W.H., Guggenheim, S., and Lin, J.-C. (1982) Rutile-type compounds. VI. Refinement of VF_2 and computer simulation of $V{:}MgF_2$. Acta Crystallographica, B38, 351–355.

Blake, R.L. (1965) Iron phyllosilicates of the Cuyuna district in Minnesota. American Mineralogist, 60, 148–169.

Chernosky, J.V. (1975) Aggreagate refractive indices and unit cell parameters of synthetic serpentine in the system MgO-Al_2O_3-SiO_2-H_2O. American Mineralogist, 60, 200–208.

Crawford, E.S., Jefferson, D.A., and Thomas, J.M. (1977) Electron-microscope and diffraction studies of polytypism in stilpnomelane. Acta Crystallographica, A33, 548–553.

Donnay, G., Morimoto, N., Takeda, H., and Donnay, J.D.H. (1964) Trioctahedral one-layer micas. I. Crystal structure of a synthetic iron mica. Acta Crystallographica, 17, 1369–1381.

Dunn, P.J., Leavens, P.B., Norberg, J.A., and Ramik, R.A. (1981) Bannisterite: New chemical data and empirical formulae. American Mineralogist, 66, 1963–1067.

Dunn, P.J., Peacor, D.R., Nelen, J.E., and Ramik, R.A. (1983) Ganophyllite from Franklin, New Jersey; Pajsberg, Sweden; and Wales: New chemical data. Mineralogical Magazine, 47, 563–566.

Dunn, P.J., Peacor, D.R., and Simmons, W.B. (1984) Lennilenapeite, the Mg-analogue of stilpnomelane, and chemical data on other stilpnomelane species from Franklin, New Jersey. Canadian Mineralogist, 22, 259–263.

Eggleton, R.A. (1972) The crystal structure of stilpnomelane. Part II. The full cell. Mineralogical Magazine, 38, 693–711.

Eggleton, R.A., and Bailey, S.W. (1965) The crystal structure of stilpnomelane. Part I. The subcell. Clays and Clay Minerals, 13, 49–63.

——— (1967) Structural aspects of dioctahedral chlorite. American Mineralogist, 52, 673–698.

Eggleton, R.A., and Chappell, B.W. (1978) The crystal structure of stilpnomelane. Part III. Chemistry and physical properties. Mineralogical Magazine, 42, 361–368.

Eggleton, R.A., and Guggenheim, S. (1986) A re-examination of the structure of ganophyllite. Mineralogical Magazine, 50, 307–315.

Forbes, W.C. (1969) Unit cell parameters and optical properites of talc on the join $Mg_3Si_4O_{10}(OH)_2$-$Fe_3Si_4O_{10}(OH)_2$. American Mineralogist, 54, 1399–1408.

Frondel, C. (1955) Two chlorites: Gonyerite and melanolite. American Mineralogist, 40, 1090–1094.

Gillery, F. H. (1959) The X-ray study of synthetic Mg-Al serpentines and chlorites. American Mineralogist, 44, 143–152.

Gruner, J.W. (1944) The composition and structure of minnesotaite, a common iron silicate in iron formations. American Mineralogist, 29, 363–372.

Guggenheim, S. (1981) Cation ordering in lepidolite. American Mineralogist, 66, 1221–1232.

——— (1984) The brittle micas. Mineralogical Society of America Reviews in Mineralogy, 13, 61–104.

——— (1986) Modulated 2:1 layer silicates (abs.). International Mineralogical Association, 14th General Meeting, 116–117.

Guggenheim, S., and Bailey, S.W. (1977) The refinement of zinnwaldite-1M in subgroup symmetry. American Mineralogist, 62, 1158–1167.

——— (1982) The superlatice of minnesotaite. Canadian Mineralogist, 20, 579–584.

Guggenheim, S., and Eggleton, R.A. (1986a) Structural modulations in Mg-rich and Fe-rich minnesotaite. Canadian Mineralogist, 24, 479–497.

——— (1986b) Cation exchange in ganophyllite. Mineralogical Magazine, 50, 517–520.

Guggenheim, S., Bailey, S.W., Eggleton, R.A., and Wilkes, P. (1982) Structural aspect of greenalite and related minerals. Canadian Mineralogist, 20, 1–18.

Hazen, R.M., and Finger, L.W. (1978) The crystal structures and compressibilities of layer minerals at high pressure. II. Phlogopite and chlorite. American Mineralogist, 63, 293–296.

——— (1982) Comparative crystal chemistry. Wiley, New York, 231 p.

Hazen, R.M., and Wones, D.R. (1972) The effect of cation substitution on the physical properties of trioctahedral micas. American Mineralogist, 57, 103–129.

Hutton, C.O. (1938) The stilpnomelane group of minerals. Mineralogical Magazine, 25, 172–206.

Jagodzinski, H., and Kunze, G. (1954) Die rollschenstruktur des chrysotils. I. Allgemeine Beugungstheorie und Kleinwinkelstreuung. Neues Jahrbuch für Mineralogie Monatshefte, 4, 95–108.

Jakob, J. (1923) Vier Mangansilikat aus dem Val d'Err (Kt Graubunden). Schweizerische Mineralogische und Petrographische Mitteilungen, 3, 227–237.

Jefferson, D.A. (1976) Stacking disorder and polytypism in zussmanite. American Mineralogist, 61, 470–483.

——— (1978) The crystal structure of ganophyllite, a complex manganese aluminosilicate. I. Polytypism and structural variation. Acta Crystallographica, A34, 491–497.

Joswig, W., Amthauer, G., and Takéuchi, Y. (1986) Neutron diffraction and Mössbauer spectroscopic study of clintonite (xanthophyllite). American Mineralogist, 71, 1194–1197.

Kato, T. (1980) The crystal structure of ganophyllite; monoclinic subcell. Mineralogical Journal (of Japan), 10, 1–13.

Kato, T., and Takéuchi, Y. (1983) The pyrosmalite group of minerals. I. Structure refinement of manganpyrosmalite. Canadian Mineralogist, 21, 1–6.

Kunze, G. (1956) Die gewellte struktur des antigorits. I. Zeitschrift für Kristallographie, 108, 82–107.

Lee, J.H., and Guggenheim, S. (1981) Single crystal X-ray refinement of pyrophyllite-1*Tc*. American Mineralogist, 66, 350–357.

Lin, J.-C., and Guggenheim, S. (1983) The crystal structure of a Li,Be-rich brittle mica: A dioctahedral-trioctahedral intermediate. American Mineralogist, 68, 130–142.

Lonsdale, P.F., Bischoff, J.L., Burns, V.M., Kastner, M., and Sweeney, R.E. (1980) A high-temperature hydrothermal deposit on the seabed at a Gulf of California spreading center. Earth and Planetary Science Letters, 49, 8–20.

Lopes-Vieira, A., and Zussman, J. (1969) Further detail on the crystal structure of zussmanite. Mineralogical Magazine, 37, 49–60.

McCauley, J.W., Newnham, R.E., and Gibbs, G.V. (1973) Crystal structure analysis of synthetic fluorophlogopite. American Mineralogist, 58, 249–254.

Mellini, M. (1982) The crystal structure of lizardite 1*T*: Hydrogen bonds and polytypism. American Mineralogist, 67, 587–598.

Muir Wood, R. (1980) The iron-rich blueschist-facies minerals: 3. Zussmanite and related minerals. Mineralogical Magazine, 48, 605–614.

Newnham, R.E. (1961) A refinement of the dickite structure and some remarks on polytypism of the kaolin minerals. Mineralogical Magazine, 32, 683–704.

Newnham, R.E., and Brindley, G.W. (1956) The crystal structure of dickite. Acta Crystallographica, 9, 759–764.

Oswald, H.R., and Asper, R. (1977) Bivalent metal hydroxides. In R.M.A.

Lieth, Ed., Preparation and crystal growth of materials with layered structures, p. 77–140. Reidel, Holland.

Ozawa, T., Takahata, T., and Buseck, P. (1986) A hydrous manganese phyllosilicate with 12 Å basal spacing (abs.). International Mineralogical Association, 14th General Meeting, 194.

Pauling, L. (1930) The structure of micas and related minerals. Proceedings of the National Academy of Sciences, 16, 123–129.

Peacor, D.R., Dunn, P.J., and Simmons, W.B. (1984) Eggletonite, the Na-analogue of ganophyllite. Mineralogical Magazine, 48, 93–96.

Perdikatsis, B., and Burzlaff, H. (1981) Strukturverfeinerung am Talk $Mg_3[(OH)_2Si_4O_{10}]$. Zeitschrift für Kristallographie, 156, 177–186.

Plimer, I.R. (1977) Bannisterite from Broken Hill, Australia. Neues Jahrbuch für Mineralogie Monatshefte, 504–508.

Radoslovich, E.W. (1961) Surface symmetry and cell dimensions of layer-lattice silicates. Nature, 191, 67–68.

——— (1963) The cell dimensions and symmetry of layer-lattice silicates. IV. Interatomic forces. American Mineralogist, 48, 76–99.

Radoslovich, E.W., and Norrish, K. (1962) The cell dimensions and symmetry of layer lattice silicates. I. Some structural considerations. American Mineralogist, 47, 599–616.

Rayner, J.H., and Brown, G. (1973) The crystal structure of talc. Clays and Clay Minerals, 21, 103–114.

Robinson, G.W., and Chamberlain, S.C. (1984) The Sterling mine, Antwerp, N.Y. Mineralogical Record, 15, 199–216.

Saalfeld, H., and Wedde, M. (1974) Refinement of the crystal structure of gibbsite, $Al(OH)_3$. Zeitschrift für Kristallographie, 139, 129–135.

Shannon, R.D. (1976) Revised effective ionic radii and systematic studies of interatomic distances in halides and chalcogenides. Acta Crystallographica, A32, 751–767.

Smith, W.C. (1948) Ganophyllite from the Benallt mine, Rhiw, Caernarvonshire. Mineralogical Magazine, 28, 343–352.

Smith, M.L., and Frondel, C. (1968) The related layered minerals ganophyllite, bannisterite, and stilpnomelane. Mineralogical Magazine, 36, 893–913.

Steadman, R., and Nuttall, P.M. (1963) Polymorphism in cronstedtite. Acta Crystallographica, 16, 1–8.

Takeda, H., and Morosin, B. (1975) Comparison of observed and predicted structural parameters of mica at high temperature. Acta Crystallographica, B31, 2444–2452.

Takéuchi, Y. (1965) Structures of brittle micas. Clays and Clay Minerals, 13, 1–25.

Takéuchi, Y., and Sadanaga, R. (1966) Structural studies of brittle micas. (I) The structure of xanthophyllite refined. Mineralogical Journal (of Japan), 4, 424–437.

Threadgold, I. (1979) Ferroan bannisterite—A new type of layer silicate structure (abs.). In Seminar on Broken Hill. Mineralogical Society of New South Wales and Mineralogical Society of Victoria.

Toraya, H. (1981) Distortions of octahedra and octahedral sheets in 1M micas and the relation to their stability. Zeitschrift für Kristallographie, 157, 173–190.

Whittaker, E.J.W. (1956a) The structure of chrysotile. II. Clinochrysotile. Acta Crystallographica, 9, 855–862.

——— (1956b) The structure of chrysotile. III. Orthochrysotile. Acta Crystallographica, 9, 862–864.

Wicks, F.J., and Whittaker, E.J.W. (1975) A reappraisal of the structures of the serpentine minerals. Canadian Mineralogist, 13, 227–243.

Zen, E. (1960) Metamorphism of lower Paleozoic rocks in the vicinity of the Taconic range in western Vermont. American Mineralogist, 45, 129–175.

Zigan, F., and Rothbauer, R. (1967) Neutronbeugungsmessungen am Brucit. Neues Jahrbuch für Mineralogie Monatshefte, 137–143.

Zigan, F., Joswig, W., and Burger, N. (1978) Die Wasserstoffpositionen im Bayerit, $Al(OH)_3$. Zeitschrift für Kristallographie, 148, 255–273.

Zussman, J. (1954) Investigation of the crystal structure of antigorite. Mineralogical Magazine, 40, 498–512.

Manuscript received July 25, 1986
Manuscript accepted April 3, 1987